

Re-evaluation of the kinematics of Victoria Block using continuous GNSS data

R.M.S. Fernandes,^{1,2} J.M. Miranda,³ D. Delvaux,^{4,5} D.S. Stamps⁶ and E. Saria⁶

¹University of Beira Interior, IDL, R. Marques d'Avila e Bolama, Covilhã, Portugal. E-mail: rmanuel@di.ubi.pt

²Faculty of Aerospace Engineering, TU Delft, Kluyverweg, 1, Delft, The Netherlands

³Instituto Português do Mar e Atmosfera IDL, Campo Grande, 1749-016 Lisboa, Portugal

⁴Royal Museum for Central Africa, B3080 Tervuren, Belgium

⁵School of Geosciences, University of the Witwatersrand, Johannesburg, South Africa

⁶Department of Earth and Atmospheric Sciences, Purdue University, West Lafayette, IN 47907, USA

Accepted 2012 November 13. Received 2012 November 4; in original form 2012 July 15

SUMMARY

The divergent boundary between the Somalia and Nubia plates is a complex tectonic domain where extensional processes are localized along narrow rift structures, isolating small blocks imbedded within the East African Rift. One of these tectonic units is the Victoria Block, which is the subject of this study. Here we process space-geodetic data for 37 permanent GNSS stations distributed along Nubia, Somalia and Victoria to (1) compute the motion of the three tectonic units in the ITRF2008 reference frame and (2) deduce the relative motion of Victoria with respect to its neighbouring plates. The Nubia Plate motion is computed from a set of 25 stations, the Somalia Plate motion from a set of 7 stations and the Victoria motion from a set of 5 stations. Although the number and distribution of the used stations is still not optimal, the good adjustment between observed and predicted motions confirms that Victoria acts as a rigid tectonic block. The instantaneous relative Euler poles for the Nubia–Victoria and Somalia–Victoria pairs are now evaluated as 10.66°N, 32.98E°, 0.120° Myr⁻¹ and 8.02°S, 32.29°E, 0.159° Myr⁻¹, respectively. The computation of the relative interplate velocities along Victoria's boundary is straightforward in most situations because the western and northeastern boundary segments correspond to well-developed rift basins, where extension is mostly normal to rift basin flanks and seismicity concentrates along narrow structures. This is particularly evident on the Western Branch between Victoria and Nubia. The southeastern limit of the Victoria Block is poorly defined, and geodetic data indicate that differential motion between Somalia and Victoria may be accommodated by a complex boundary area, which roughly encompasses the Masai Terrain. Geodetic observations of the Victoria–Somalia boundary along the Eastern Branch, particularly in the Manyara Rift, reveal highly oblique horizontal extension. In this region seismicity is sparse which suggests that strain is accommodated by magmatic processes.

Key words: Satellite geodesy; Plate motions; Continental neotectonics; Africa.

1 INTRODUCTION

The East African Rift (EAR) system extends for more than 5000 km across Africa and is often used as a natural laboratory for the study of continental rifting at an early stage (e.g. Nicholas *et al.* 1994; Calais *et al.* 2008; Corti 2009; Delvaux & Barth 2010 and references therein). Space geodesy has contributed to the understanding of this complex tectonic system by providing direct measurements of surface displacement, permitting the identification and characterization of the present-day kinematics of the two major lithospheric plates that diverge across the EAR: the Nubia (NUBI) and Somalia (SMLA) plates, and the complex tectonic system between them

(e.g. Sella *et al.* 2002; Fernandes *et al.* 2004; Prawirodirdjo & Bock 2004; Stamps *et al.* 2008). When the observation period of geodetic measurements at stable sites is sufficient to produce velocities with 95 per cent uncertainties smaller than the velocity itself, typically a 3.5-yr minimum period for continuous GPS (Blewitt & Lavallee 2002), they can be used for robust kinematic interpretations that can be compared with geological observations.

Within the Nubia–Somalia boundary domain there are a number of lithospheric blocks surrounded by active rift structures with known geological and/or seismic signatures (*cf.* Fig. 1). Calais *et al.* (2006) used GPS observations and earthquake slip vectors to show that two of these blocks should be interpreted as additional tectonic

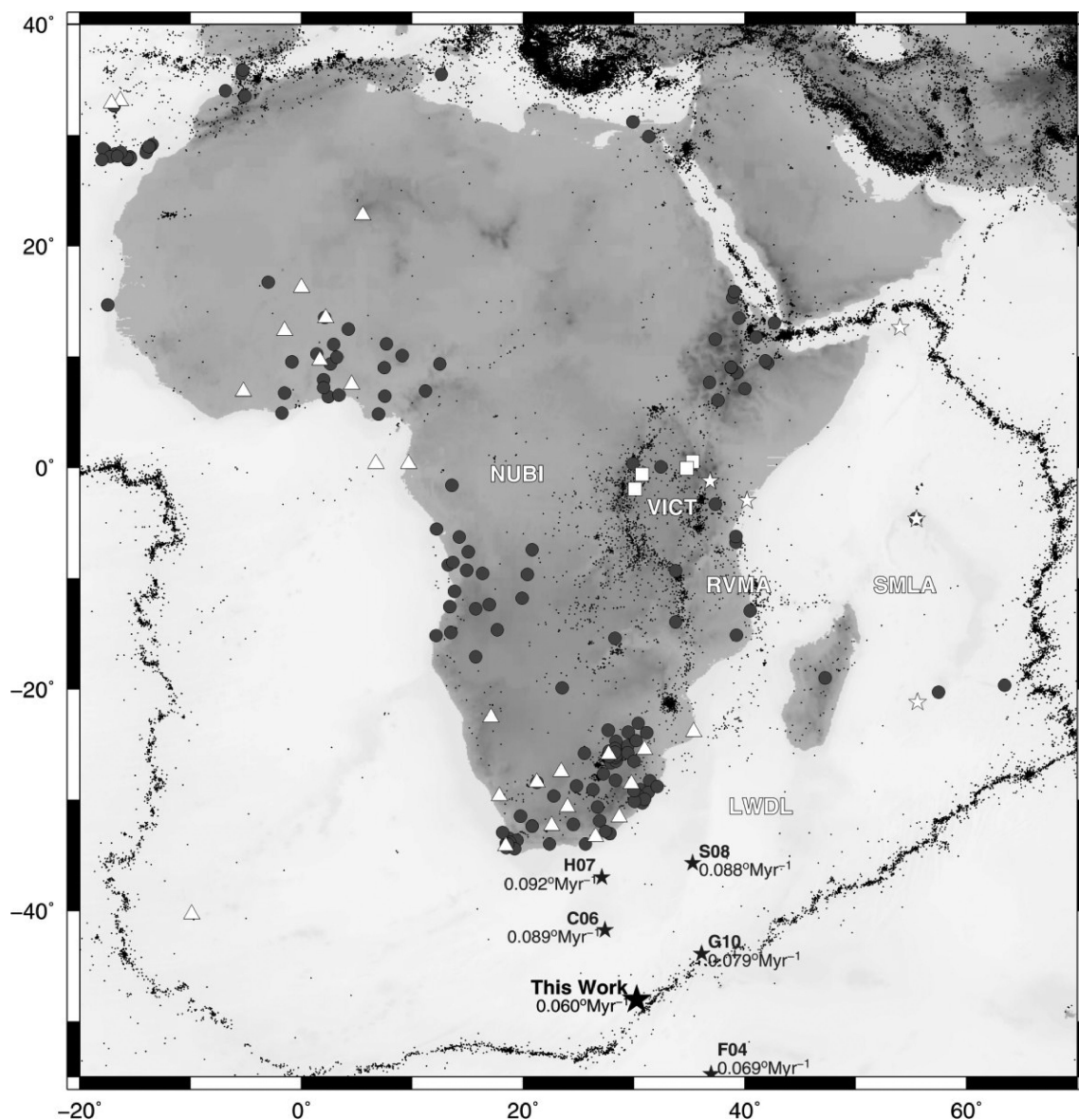


Figure 1. Seismicity for the studied area (IRIS 2011) roughly defining the limits of the three studied plates: Nubia (NUBI), Somalia (SMLA) and Victoria (VICT). The approximate locations of Rovuma (RVMA) and Lwandle (LWDL) are also indicated. GNSS stations used on the computation of the angular velocities are white—triangles (Nubia), stars (Somalia) and squares (Victoria). The dark circles indicate stations excluded from the analysis (see text for more details). The locations of the Somalia–Nubia relative Euler pole are also indicated as dark stars for this work and other previous published solutions: F04, Fernandes *et al.* (2004); C06, Calais *et al.* (2006); H07, Horner-Johnson *et al.* (2007); S08, Stamps *et al.* (2008); G10, Argus *et al.* (2010).

blocks (Victoria, Rovuma) and quantified the angular rotation of the Victoria Block. Based on plate closure, Horner-Johnson *et al.* (2007) determined the existence of the Lwandle Block, also shown in Fig. 1, and calculated the angular velocity from spreading rates and transform fault azimuths. Stamps *et al.* (2008) derived the first complete kinematic model of the EAR by inverting space-geodetic solutions with other geophysical data (spreading rates, earthquake slip vectors and transform-fault azimuths) to support the interpretation of the three above-mentioned tectonic blocks and to derive consistent angular velocities for the whole set.

The objective of this work is to focus on the best defined of these units, the Victoria Block, which has been referenced as Victoria (Kaz'min *et al.* 1987) and Ukerewe (Hartnady 2002). Previously, its limits could not be defined by space-geodetic methods alone due to limitations in the spatial coverage of the GNSS stations. Calais

et al. (2006) hypothesized that the Victoria Block is formed by the Tanzania Craton and bounded by two branches (Western and Eastern) of the EAR. The Victoria–Rovuma tectonic boundary is poorly defined, but may correspond with the Usangu-Ruaha, Kilombero and the Ruhuhu rifts, which were interpreted by LeGall *et al.* (2004) as the southern link between the Eastern and Western rift branches to the southeast of the Tanzania Craton.

In recent years the quantity and quality of continuous GNSS stations has increased gradually in East Africa, hence improving the capability of space-geodetic data to decipher the deformation patterns of the Victoria boundaries. To do so, we reassess the angular velocities of the Nubia and Somalia plates using a new set of derived-GNSS position solutions based exclusively on continuous GNSS stations and using the latest realization of the International Terrestrial Reference System: ITRF2008 (Altamimi *et al.* 2011).

We compute the motion of Victoria with respect to its neighbouring plates (Nubia and Somalia) and we discuss the implications of the obtained solutions on the rifting geometry at this segment of the EAR.

2 REGIONAL SETTING

South of the Main Ethiopian Rift, which marks the northern segment of the Nubia–Somalia Plate boundary across the East African Plateau, there is a marked increase in the tectonic complexity of the domain lying between these two large plates. The EAR splits into two branches (cf. Fig. 2), the Western Branch, characterized by higher magnitude, deeper seismicity (Yang & Chen 2010; Lindenfield & Rumpker 2011) and relatively small amounts of volcanic activity (Ebinger 1989) compared to the Eastern Branch, which has voluminous magmatic activity and shallower, lower mag-

nitude seismicity (e.g. Albaric *et al.* 2009). The Western Branch comprises the Albertine and Kivu rifts in the northwest and the Tanganyika–Rukwa–Malawi rift system in the southwest (cf. Fig. 2). The Eastern Branch is formed by the north–south oriented Kenya Rift which splays southwards in the North Tanzanian Divergence zone in three smaller rift segments: Eyasi, Manyara and Pangani Rifts (LeGall *et al.* 2004). The Manyara segment continues southwards to the Dodoma region (Macheyeki *et al.* 2008) and joins the Kilombero and Ruaha–Usangu Rift system through which makes the Western and Eastern Branches connection with the Western Branch in the Rungwe Volcanic Province (Ebinger 1989). The Kilombero Rift is interpreted as the reactivation of previous Karoo (Permo-Triassic) rifting episodes associated with the Pangea breakup (Delvaux 2001; LeGall *et al.* 2004).

The two branches, located between 2°N and 10°S, bound an approximately 1000 m high, 1.3 million km² topographic plateau that corresponds approximately to the Tanzania Craton. The

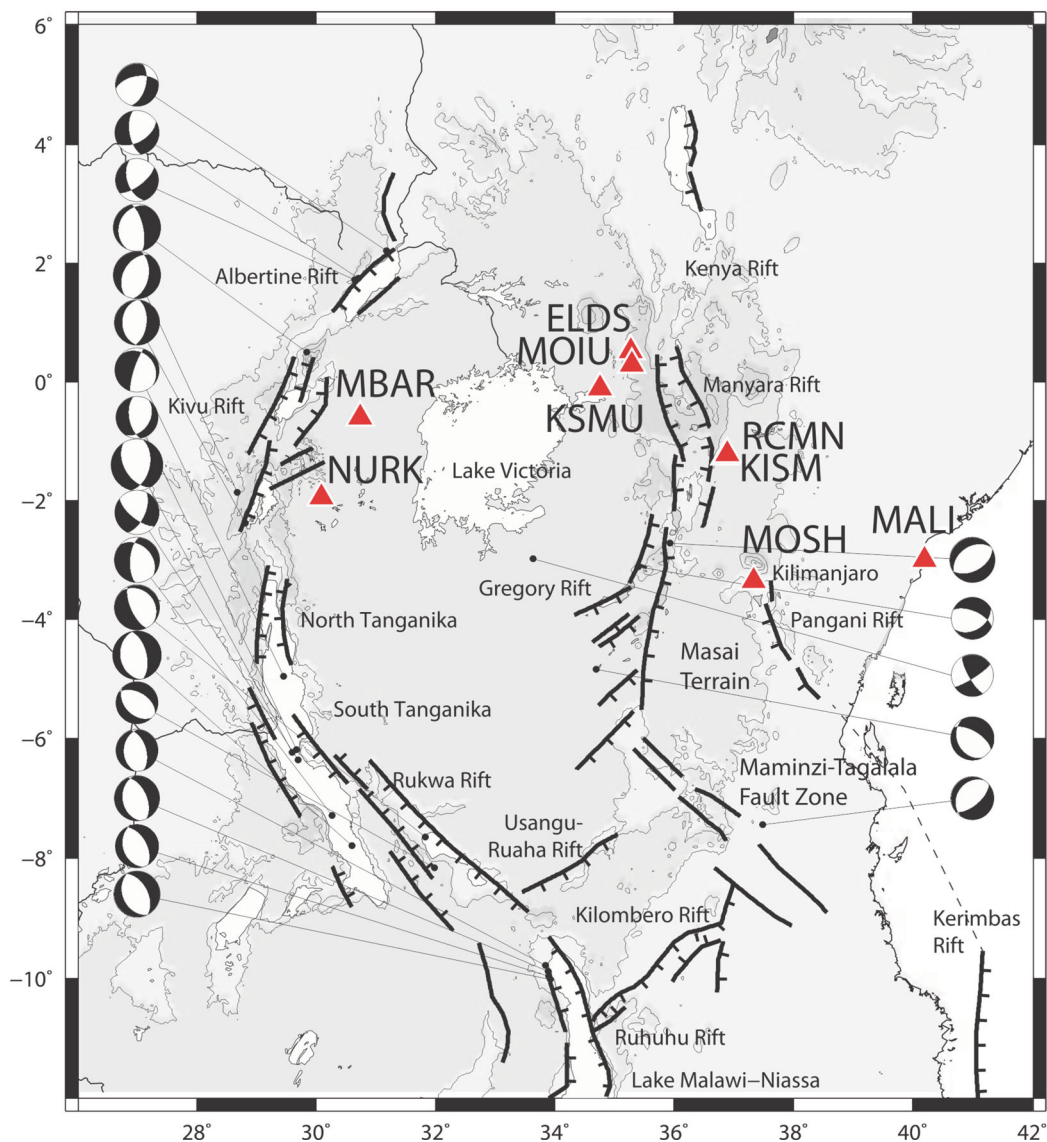


Figure 2. Tectonic sketch of Victoria Block GNSS stations used on the computation of the angular velocity for Victoria and other stations discussed in the text are marked with triangles. Focal mechanisms from Global CMT catalogue (Global CMT 2011) for the period 1976–2011 and magnitude larger than 5.5. Geological sketch adapted from LeGall *et al.* (2004) and Delvaux & Barth (2010). The 1000 m contour (darker grey) approximately defines the Tanzanian Plateau.

Tanzania Craton is formed by an old lithosphere composed of relatively undisturbed Archean to early Proterozoic terranes and is surrounded by remnants of Palaeoproterozoic to Neoproterozoic mobile belts (Kaz'min *et al.* 1987; Delvaux 2001; Weeraratne *et al.* 2003). Present-day rifting associated with the Victoria Block follows these pre-existing structures (e.g. Corti 2009).

While Cenozoic rifting in the EAR initiated ~ 40 Ma with volcanism in the Turkana Rift (George *et al.* 1998), its propagation into southern Kenya is younger than 25 Myr. At the latitude of the Tanzania Craton, rifting propagated southward from 12 Myr in Western Branch (Ebinger 1989) and after 5 Myr along the Eastern Branch (Macheyeki *et al.* 2008). The southward expansion of the Manyara Rift within the Eastern Branch began even later at about 1.2 Ma (Macheyeki *et al.* 2008).

Focal mechanisms of large earthquakes have been used to characterize the stress regime along the different boundary domains of Victoria and show that the Eastern and Western Branches are in overall E–W extension (Foster & Jackson 1998; Brazier *et al.* 2005; Delvaux & Barth 2010; Yang & Chen 2010). In the northern Western Branch, most earthquakes of the events are dip-slip with an ESE extension, normal to the Kivu Rift system.

Along the southern Western Branch and the Rukwa Rift, earthquake focal mechanisms show dominantly normal faulting but strike-slip mechanisms are also present (Brazier *et al.* 2005; Delvaux & Barth 2010). Field structural investigations show that faulting in the Rukwa Rift during the Late Cenozoic are pure normal dip-slip type (Delvaux *et al.* 2012), but the regime changes rapidly into strike-slip faulting in the Rungwe volcanic area at the junction between the Rukwa and Malawi Rifts (Delvaux *et al.* 1992). On the northeastern border of the Victoria Block there is evidence for distributed block deformation close to the North Tanzania Divergence where the Eastern Branch follows the poorly defined margin between the Tanzania Craton and the Mozambique Belt, with approximately E–W extension (Brazier *et al.* 2005; Macheyeki *et al.* 2008; Delvaux & Barth 2010).

Calais *et al.* (2006) combined GPS data and earthquake slip vectors to derive the first estimate of the counter-clockwise relative motion between Victoria and Nubia. Stamps *et al.* (2008) determined a new pole of rotation for VICT–NUBI using also geological data at $8.370^\circ\text{N}/32.589^\circ\text{E}/0.1294^\circ/\text{Myr}$. Their result corresponds to a counter-clockwise rotation of the Victoria Block relative to Nubia with a constant increment of the relative velocity along the western boundary of the Victoria Block from approximately 1 mm yr^{-1} in the north up to 4 mm yr^{-1} in the south at the Nubia–Victoria–Rovuma Triple Junction. The instantaneous pole of rotation between Victoria and Somalia computed by Stamps *et al.* (2008) is located at $9.319^\circ\text{S}/33.538^\circ\text{E}/0.2024^\circ/\text{Myr}$ resulting in a decrease of the relative velocity along the eastern Victoria boundary from approximately 5 mm yr^{-1} in the north up to less than 1 mm yr^{-1} in the south. Both rotation poles indicate counter-clockwise motion of Victoria with respect to both Nubia and Somalia and the localization of the larger strain rates in the southern sector of the Western Branch and in the northern sector of the Eastern Branch.

LeGall *et al.* (2004) interpreted the complex tectonics of the Kilombero area as the spatial link between both the Western and Eastern Branches of the EAR south of the Tanzania Craton. However, the instantaneous rotation pole computed by Stamps *et al.* (2008) for Rovuma, corresponds to a clockwise motion of this block with respect to Nubia and Somalia, and suggests differential motion between Victoria and Rovuma along the southern border of Victoria. The differential motion across the Kilombero area indicated by Stamps *et al.* (2008) combined with low seismicity (Foster

& Jackson 1998; Yang & Chen 2010) suggests the Kilombero area is indeed the southeastern boundary of the Victoria Block.

3 METHODOLOGY

Fig. 1 shows the distribution of the continuous GNSS stations evaluated in this work. The total number of permanent stations in Africa for which we are able to compute daily solutions is greater than 200 stations. This includes some stations that are no longer available but which time-series are long enough to provide useful information (e.g. MALI—Malindi, Kenya). However, the majority of existing stations in Africa still have short observation periods (installed in the last 2–3 yr) and/or have significant gaps. Therefore, in some cases, the derived time-series resembles campaign solutions, mainly due to communication problems even if no reinstallation/replacement of receiver and/or antenna has occurred.

Our data sets were mainly retrieved from international data centres, namely CDDIS (<http://cddis.nasa.gov/>), UNAVCO (<http://www.unavco.org/>) and AFREF (<ftp://ftp.afref.org/>). In addition to these data sets, some of our local partners, whose data are not publicly available, provided observations that permitted to densify the number of solutions in our area of interest, for example, KSMU, ELDS, MOSH and SCTR.

To compute the position time-series, we first compute daily solutions using the GIPSY-OASIS II version 5.0 software package (Webb & Zumberge 1995) with the PPP—Precise Point Positioning strategy (Zumberge *et al.* 1997). In a second step, the ambiguities were attempted to be fixed using AMBIZAP (Blewitt 2008). This application permits us to process large networks by estimating the integer ambiguity values using optimized linear combinations of pairs of stations.

Finally, the alignment into ITRF2008 of the daily solutions was carried out by estimating a seven-parameter Helmert transformation using more than 100 IGS stations globally distributed as reference. The core of this reference network is the set of IGS08 stations (Reischung *et al.* 2011) added with some former IGS stations to maintain the consistency of the reference network as well as possible through the years (since 1996). We limited the estimation of the initial velocity field to stations located on the assumed stable part of the tectonic blocks and with a sufficient long data span: >3.0 yr for Nubia and >2.0 yr for Somalia and Victoria.

The computation of the velocity field was carried out with the procedures described by Bos *et al.* (2008), using the time-series analysis service that is publicly available at <http://www.geodac.net>. A linear trend is estimated, together with a seasonal signal when the data span is longer than 3 yr as well as identified jumps (offsets) in the North, East and Up components. The epochs for the detected offsets are included to also estimate their magnitude in the three components during the analysis. The estimation of the associated uncertainty takes into account the temporal correlation of the observations assuming a white plus power-law noise model for which the values of the variances and the spectral index were computed during the estimation process. Although this approach inhibits the explicit computation of correlations between the different components of each velocity, it reflects more properly the real errors on the velocity estimation (the values are increased by factors of 5–10) since the associated uncertainties are not only based on the formal errors.

Finally, we performed an iterative process to compute the angular velocities for each block individually. We used the same algorithm developed by DeMets *et al.* (1990) to compute NUVEL-1. In this

Table 1. Continuous GNSS stations used for the computation of Nubia, Somalia and Victoria motion with respect to ITRF2008.

	SITE	Longitude	Latitude	Initial date	Final date	Processed days	V_E (mm yr ⁻¹)	V_N (mm yr ⁻¹)
Nubia	BWES	22.57356	-32.34738	05-07-2004	24-09-2011	2210	16.71 ± 0.52	18.84 ± 0.24
	DEAR	23.99264	-30.66520	01-09-2000	24-09-2011	2668	16.85 ± 0.20	18.89 ± 0.16
	DJOU	1.66163	9.69207	24-08-2005	13-05-2009	1315	20.71 ± 0.42	19.33 ± 0.63
	GAO1	-0.00601	16.25211	29-08-2005	13-07-2009	1225	20.19 ± 0.35	19.57 ± 0.47
	GOUG	-9.88072	-40.34883	14-08-1998	18-09-2008	2618	21.36 ± 0.42	18.23 ± 0.34
	GRHM	26.50718	-33.32006	01-01-2006	30-06-2011	1725	15.14 ± 0.35	18.88 ± 0.37
	HARB	27.70724	-25.88696	12-08-2000	24-09-2011	3857	17.69 ± 0.16	18.56 ± 0.10
	INHB	35.38327	-23.87115	10-11-2007	23-09-2011	478	16.72 ± 2.00	17.69 ± 1.00
	KMAN	23.43248	-27.46078	17-04-2002	31-05-2011	2955	17.67 ± 0.37	18.80 ± 0.17
	LSMH	29.78149	-28.55765	12-01-2002	30-06-2011	2640	16.34 ± 0.21	18.26 ± 0.16
	NKLG	9.67212	0.35391	31-03-2000	24-09-2011	3885	22.25 ± 0.32	19.12 ± 0.11
	NMEY	2.18319	13.47926	29-05-2005	13-10-2009	1541	21.44 ± 0.45	19.64 ± 0.32
	NSPT	30.97517	-25.47534	10-03-2001	30-06-2011	3109	17.26 ± 0.17	17.89 ± 0.26
	OUAG	-1.51250	12.35639	30-05-2006	04-10-2009	1145	20.66 ± 0.58	18.81 ± 0.42
	PSAN	-16.33790	33.08557	27-03-2006	19-09-2009	1085	14.08 ± 0.71	17.04 ± 0.43
	RECT	4.52447	7.50549	21-07-2007	03-04-2011	501	21.22 ± 0.75	19.10 ± 0.39
	RIBJ	-17.16047	32.84537	27-03-2006	22-09-2009	1042	14.18 ± 0.55	16.75 ± 0.32
	SBOK	17.87921	-29.66933	23-08-2000	16-06-2011	3288	17.89 ± 0.17	19.30 ± 0.15
	SIMO	18.43958	-34.18794	09-08-2001	02-01-2009	1371	16.83 ± 0.53	19.24 ± 0.28
	STMP	6.73749	0.34453	25-10-2006	24-09-2011	388	21.39 ± 0.56	18.97 ± 0.26
TAMP	5.52964	22.79265	01-03-2004	22-10-2007	1119	20.37 ± 0.74	19.00 ± 0.39	
UMTA	28.67250	-31.54877	24-07-2000	25-06-2011	2855	16.19 ± 0.20	18.3 ± 0.19	
UPTN	21.25587	-28.41365	17-04-2002	27-09-2007	1411	18.02 ± 0.43	19.14 ± 0.21	
WIND	17.08943	-22.57492	12-02-2007	16-01-2011	1374	19.11 ± 0.51	19.37 ± 0.23	
YKRO	-5.24009	6.87056	18-07-1999	21-12-2010	758	21.89 ± 0.18	18.34 ± 0.25	
Somalia	KISM	36.85668	-1.25021	20-04-1998	19-03-2007	492	27.35 ± 1.56	17.91 ± 0.43
	MAL2	40.19414	-2.99606	10-07-2008	24-09-2011	1140	26.31 ± 0.66	16.33 ± 0.53
	MALI	40.19440	-2.99591	07-01-1996	11-09-2008	4275	27.32 ± 0.28	16.12 ± 0.13
	RCMN	36.89348	-1.22083	20-03-2007	13-01-2011	1145	25.49 ± 0.41	16.47 ± 0.20
	REUN	55.57172	-21.20823	14-04-1999	10-04-2009	2161	18.79 ± 0.54	11.45 ± 0.21
	SCTR	54.00597	12.64779	01-03-2008	20-01-2011	646	29.56 ± 0.77	12.51 ± 0.93
	SEY1	55.47940	-4.67372	23-01-1996	24-09-2011	3052	25.64 ± 0.35	12.83 ± 0.43
Victoria	ELDS	35.27716	+0.51871	01-05-2001	11-02-2007	188	24.99 ± 1.59	18.06 ± 1.38
	KSMU	34.75614	-0.10407	10-03-2002	12-05-2008	591	24.75 ± 0.69	18.55 ± 0.89
	MBAR	30.73788	-0.60147	17-07-2001	24-09-2011	2441	25.19 ± 0.45	17.85 ± 0.52
	MOIU	35.29001	+0.28832	15-11-2008	24-09-2011	890	23.47 ± 0.69	17.68 ± 0.61
	NURK	30.08968	-1.94455	05-12-2008	24-09-2011	975	26.10 ± 1.92	17.18 ± 1.25

process, we have excluded some stations presenting unusually high-velocity residuals that were not compatible with the expected motions. In particular, we have excluded stations with residuals greater than 1.5 mm yr⁻¹ (using an iterative process where we excluded the one with largest value of the residual at each iteration). We attribute these residuals to different reasons. At some stations the computed magnitude of identified jumps due to known equipment replacement or unknown reasons may have unaccounted for errors. We also did not exclude local problems (e.g. monument stability) at some of the locations. In the case of Nubia, we were even stricter on the accepted residuals (<1 mm yr⁻¹), in particular for the stations in South Africa due to the large number of available stations in this region (*cf.* Fig. 1). We decided to only include some of the South African stations on our computation instead of the entire data set. If we have used the same criteria as applied in the other regions (data span larger than 3 yr) the final solution would be biased by the large concentration of stations in this part of the continent. All stations removed during our iterative processed as well as their residuals with respect to the predicted velocities are listed in Table S1. Table 1 shows the final list of velocities used to compute the angular velocities for Nubia, Somalia and Victoria, respectively.

4 KINEMATICS OF VICTORIA BLOCK

The estimated angular velocities with respect to the ITRF2008 global reference frame are presented in Table 2. ITRF2008 is by definition a no-net-rotation frame (Altamimi *et al.* 2011). Consequently, the predicted velocity at each point on the Earth's surface can be considered as representative of their absolute motion on a global frame. To know the relative motions between the three discussed tectonic block pairs is necessary to differentiate the values presented in Table 2. Their representation using Euler poles are shown in Fig. 1 (for the pair Nubia–Somalia) and in Fig. 4 (for the pairs Nubia–Victoria and Somalia–Victoria).

The comparison between the relative motion across the Victoria boundary and its relationship with rifting as measured by tectonics is easily done along the Western Branch, where rifting is focused and the tectonic boundary is marked by well-defined rift basins. However this is more difficult to achieve along the southeast border between Victoria and Somalia, because of the low level of seismicity and poor morphological expression, and therefore it cannot be used to detect active rift processes; even if the geometry of the rift basins does not point to a focused boundary. Fig. 3 presents the comparison between the velocity estimate for eight stations and what should be

Table 2. Angular velocity estimates and associated angular uncertainties for Nubia, Somalia and Victoria expressed with respect to ITRF2008.

Plate	Angular velocity			Uncertainties					
	X	Y	Z	σ^2_X	σ^2_Y	σ^2_Z	σ_{XY}	σ_{XZ}	σ_{YZ}
NUBI	$+0.56102 \times 10^{-3}$	-0.29779×10^{-2}	0.34882×10^{-2}	0.47343×10^{-9}	0.94129×10^{-10}	0.16055×10^{-9}	0.14305×10^9	-0.16322×10^{-9}	-0.57559×10^{-10}
SMLA	-0.39629×10^{-4}	-0.33283×10^{-2}	0.42611×10^{-2}	0.58963×10^{-8}	0.51712×10^{-8}	0.77524×10^{-9}	0.53123×10^{-8}	-0.54160×10^{-9}	-0.50817×10^{-9}
VICT	$+0.22823 \times 10^{-2}$	-0.18612×10^{-2}	0.38743×10^{-2}	0.12051×10^{-5}	0.50700×10^{-6}	0.25520×10^{-8}	0.77859×10^{-6}	-0.73528×10^{-8}	-0.47607×10^{-8}

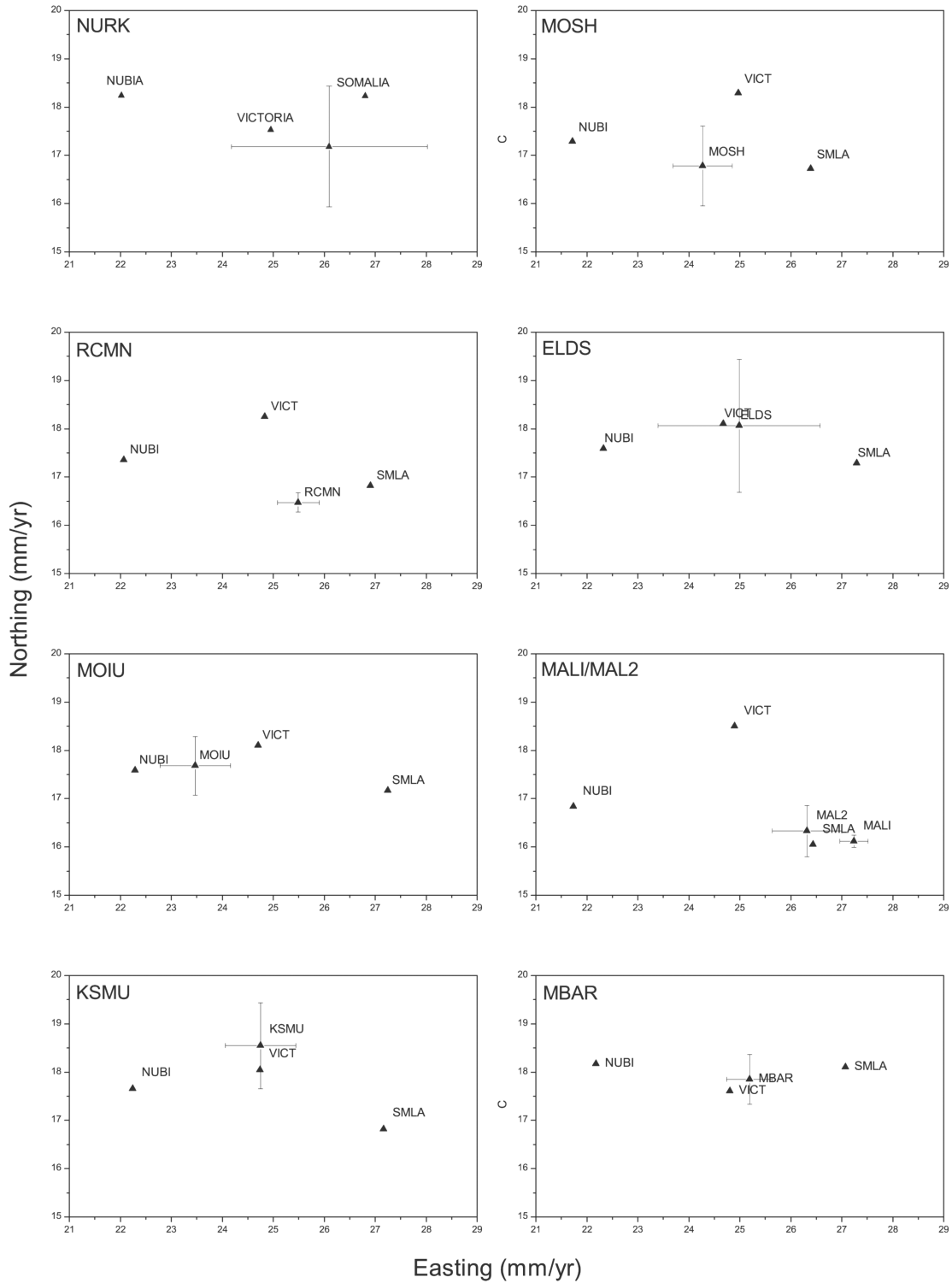


Figure 3. Comparison between the estimated velocities (with 1- σ uncertainty) for the stations in the Victoria region and the predicted rigid body velocity computed for the three tectonic blocks: Nubia, Somalia and Victoria.

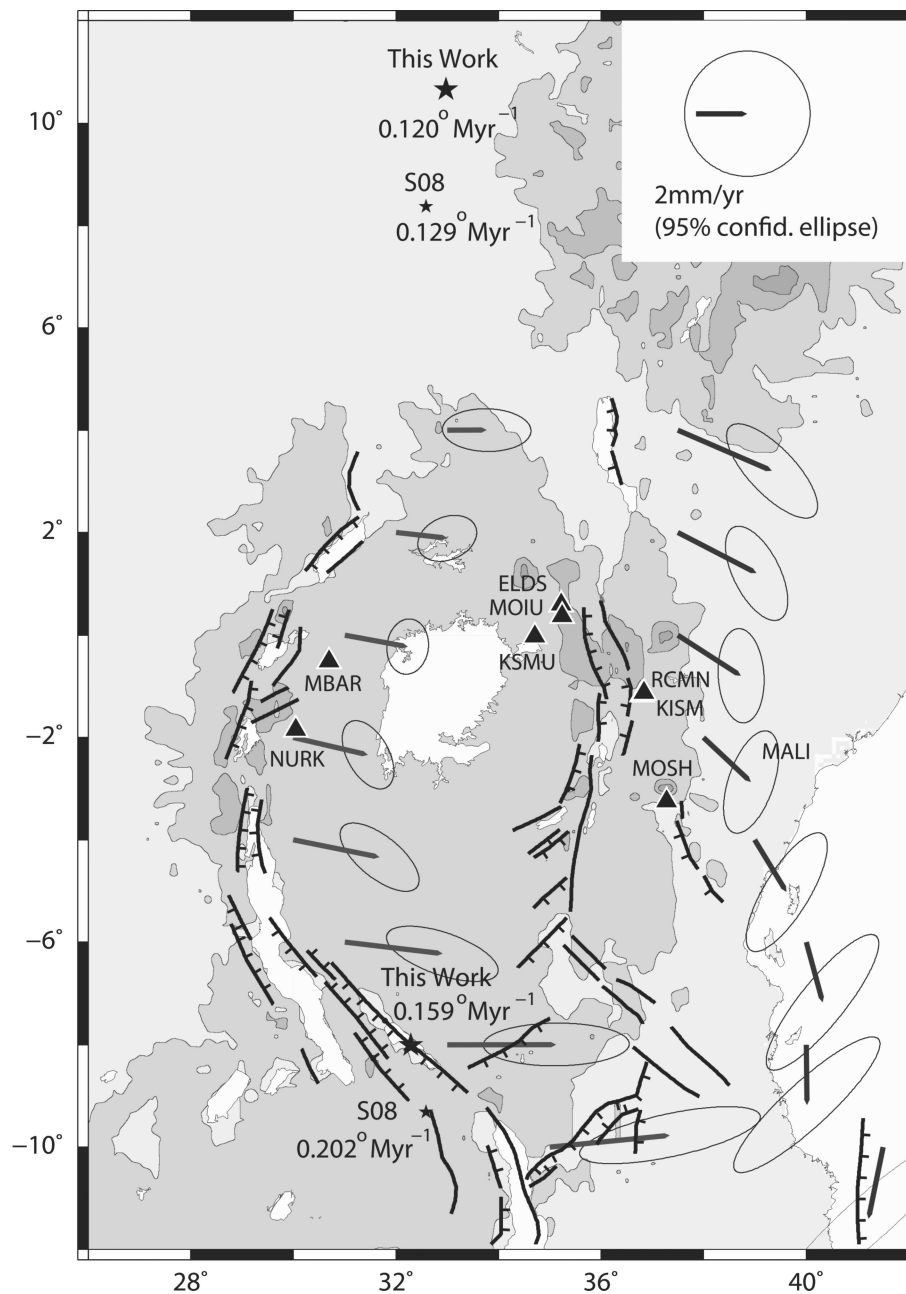


Figure 4. Location of the rotation poles for Nubia–Victoria and Victoria–Somalia plate pairs. Small black stars indicate the determinations made by Stamps *et al.* (2008). Relative motions represented by dark grey vectors along the Nubia–Victoria plate boundary are referred to fixed Nubia, while relative motions along the Victoria–Somalia plate boundary are relative to fixed Victoria.

measured in case it was attached to rigid Nubia, Somalia or Victoria. It can be observed that, within the accuracy limits, ELDS, KSMU, MBAR and even NURK are in good agreement (within 95 per cent confidence intervals) with the kinematic parameters deduced for Victoria and that MALI/MAL2 is coherent with Somalia mean motion (*cf.* Fig. 2 for locations). A different situation arises for MOSH, that moves with an intermediate velocity between Victoria and Somalia. The RCMN/KISM pair was used to compute the pole for Somalia since their residuals were within the threshold value. However, they also present velocities that are not completely compatible with Somalia (*cf.* Fig. 3). This can be interpreted as a consequence of their location in the interblock deformation domain

and so, we hypothesize that the Masai Terrain is mostly attached to the Victoria Block.

The uncertainties due to the relatively short data spans and/or the existence of data gaps are evident when we compare the time-series for ELDS and MOIU (see Supporting Information). ELDS has a longer data span but has significant data gaps whereas the time-series for MOIU is still short (less than 3 yr, *cf.* Table 1). The magnitude of the differences in the estimated motion, 0.4 mm yr^{-1} and 1.5 mm yr^{-1} in North and East component, respectively, are likely due to observational errors rather than due to real physical signals. Hence the real uncertainty associated with the motions for these stations is expressed in the estimated uncertainties since they

are larger than the differences between the velocities of the two stations.

Fig. 4 shows the location of the relative rotation poles for Victoria–Nubia and Victoria–Somalia, as well as the relative velocities along the Western and Eastern rift branches. Note that these velocities are not referred to the same referential: the velocities along the western border are relative to fixed Nubia, while the velocities along the eastern border are referred to fixed Victoria.

Along the Western Branch, relative linear velocity shows a continuous southward increase between 2.0 mm yr^{-1} , with N96E direction, close to the Albertine Rift, up to 4.3 mm yr^{-1} with N90E direction, in the southern tip of Rukwa Rift. Along the Eastern Branch, relative linear velocity shows a continuous southward decrease between 4.0 mm yr^{-1} , with N113E direction, close to the Kenya Rift down to 2.3 mm yr^{-1} , with N160E direction, on the eastern border of the Masai Terrain. The comparison between the velocity computed by the space-geodetic techniques and the determination made by tectonic methods (Ebinger 1989) is impossible, because rifting processes have not been stable during the whole geological period, as shown by Macheyeke *et al.* (2008) and Delvaux *et al.* (1992).

5 DISCUSSION AND CONCLUSIONS

Data presented here are the result of re-processing of GNSS permanent stations covering Nubia, Somalia and Victoria using the ITRF2008 reference frame. The time-series for each station have a sufficient data span to ensure an improvement with respect to previous determinations of Victoria motion (Fernandes *et al.* 2004; Calais *et al.* 2006; Stamps *et al.* 2008). We did not take into account elastic strain accumulation close to the tectonic boundaries because most geodetic sites are located more than 100 km away from them. The exceptions are RCMN and KISM stations located close to Nairobi, approximately 50 km away from Manyara Rift, which were used in the computation of the Somalia angular velocity. We use RCMN and KISM in the final solutions due to the still small number of GNSS stations with observations long enough to provide an accurate computation of the Somalia mean velocity. The number of individual solutions for Somalia, seven solutions at five distinct locations, did not increase significantly with respect to the stations used in previous solutions (e.g. Fernandes *et al.* 2004; Calais *et al.* 2006; Stamps *et al.* 2008; Argus *et al.* 2010). However, the use of a station in the northern tip of the Somalia plate (SCTR—Socotra) provides an important constraint on the Somalia Plate motion that was not available for the previously published solutions. The removal of the pair RCMN/KISM would imply an average increment of $\sim 0.2 \text{ mm yr}^{-1}$ on the opening of Somalia with respect to Nubia (and Victoria). The use of both stations for Somalia solution does not tightly constrain the solution for Somalia since, as shown in Fig. 3, RCMN/KISM (and also MOSH) still present velocities that are transitional between Somalia and Victoria.

We compare in Fig. 1 our computed relative pole between Somalia and Nubia with several other solutions. All solutions are concentrated near the Southeast Indian Ridge which implies minimal, if any, relative deformation in this area (which, assuming the existence of the Lwandle Block is also no point of contact between Nubia and Somalia). The major implication of our solution for the Somalia–Nubia pair is a smaller rate (5.7 mm yr^{-1} with azimuth S82E at 10°N ; 40°E) of the opening in the Afar region (but consistent in azimuth with the Ethiopian Rift) than the previous studies.

Geodetic data provide information concerning the limits of the plates, interpreted as rigid blocks, in particular regarding the Victoria Block. Clearly its western boundary follows a succession of seismically active rift basins that separate Nubian from Victorian velocities, and Manyara Rift bounds the eastern margin up to the latitude $\sim 3^\circ\text{S}$. South of this limit interplate deformation is accommodated by a complex system of normal faults which encompass the Masai Terrain. This is consistent with the tectonic interpretation made by LeGall *et al.* (2004) where the Pangani Rift meets the Kerimbas Rift offshore through an oblique fault which could be interpreted as a very slow right-lateral dextral strike-slip fault ($\sim 2 \text{ mm yr}^{-1}$, *cf.* Fig. 4). We suggest this structure corresponds to the southeastern boundary of the Victoria Block.

Delvaux & Barth (2010) inverted focal mechanisms to compute the mean direction of horizontal extension on most of the segments along the Victoria Block boundaries, which can be directly compared with the rigid block motion parameters presented here. Along the Western Branch geodetic and seismic data compare relatively well for the Albertine Rift (N096E and N121E, respectively), Kivu Rift (N100E and N128E) and North Tanganyika (N101E and N84E) but large deviations exist along the South Tanganika (N097E and N052E) and Rukwa Rift (N090E and N035E). In the Eastern Branch along the Manyara Rift segment there is a significant difference between both determinations (N123E and N073E; Delvaux & Barth 2010); a previous determination made by Macheyeke *et al.* (2008) for Manyara Rift pointed also to a similar result (N080E).

Rifting direction deduced from geodetic data is mostly orthogonal between Albertine and Kivu rifts, but to the south, particularly along the Rukwa Rift, the obliquity between the interblock velocity and the rift flanks is large (*cf.* Fig. 4). This finding supports the Delvaux & Barth (2010) inversion of seismic data and Delvaux *et al.* (2012) inversion of geological data that suggest the Rukwa Rift basin is under orthogonal opening. In the Eastern Branch there is also large apparent obliquity on the Manyara Rift segment, as the rift flanks, the morphological expression of the rift basin and even the inversion of focal mechanism data point to $\sim\text{N075E}$ extension, while the relative interblock velocity is in the N123E direction. The results of focal mechanism inversion, which are corroborated by the morphological expression of the rift segments, suggest that the movement of Victoria cannot be expressed by a simple rigid body in this boundary or the importance of local (magmatic) processes is large as a driven mechanism for rifting.

Geodetic determinations of extension rates when extrapolated to the ages determined for the initiation of rifting systematically point to rates larger than those deduced from the analysis of fault geometry by a factor ~ 2 . Similar results were obtained in previous works (e.g. Calais *et al.* 2006) and attributed to variations in extension rates, probably lower during the early stages of rifting. However we cannot discard the influence of the *a priori* geometrical modulation used for the computation of finite extension (e.g. Ebinger 1989) and the difficulty in establishing the age for rifting initiation in the different segments of the tectonic boundary.

The location of the Nubia–Victoria instantaneous rotation pole implies southward increase of the relative velocity along the Western Branch if we assume that Victoria Block is mostly rigid. This means the Rukwa Rift is presently extending with a rate more than twice the Albertine Rift. This result is compatible with the suggestion of Kaz'min *et al.* (1987) and Roberts *et al.* (2012) that rifting has developed northwards along the western margin of the Victoria Block, although active propagation is not strictly

required to explain our kinematic northward decrease of the rifting rate. Along the Eastern Branch the relative velocity between Victoria and Somalia decreases significantly from focused, magma-assisted rifting along Kenya and Manyara rifts, to a distributed deformation zone further south into the North Tanzania Divergence Zone. Once again, this is compatible with, but does not necessarily imply, a southward propagation of the Manyara Rift segment (Macheyeki *et al.* 2008).

The Victoria Block and its geodynamic behaviour in Cenozoic times is the result of continental rifting on an uplifted East Africa plateau that encompasses relatively undisturbed Archean to early Palaeoproterozoic terranes. The development of the plateau began approximately ~ 23 Ma, in early Miocene times (Ebinger 1989) when similar processes took place in other areas of the Nubia boundaries (e.g. Azores, see Luis & Miranda 2008), and much earlier than the rifting itself. From 12–15 Ma to 8 Ma, the EAR interacted with the plateau, and rifting developed close to the western flank of the plateau. The oldest volcanic expression has been identified in the Turkana Rift 40–54 Ma with the onset of rifting ~ 20 Ma later (Ebinger 1989, Ebinger *et al.* 1993; George *et al.* 1998; Roberts *et al.* 2012), but the width of the rift basins is larger in the south, consistent with the present-day geodetic extension rates. After 5 Myr rifting also developed south of the Kenya Rift. The Kenya Rift cuts into the plateau, it defines part of the eastern flank of the Victoria tectonic block, and it affects the distribution of the extension rates along the Western Branch, which became larger in the south than in the north.

The different segments of the Western Branch are largely amagmatic and they are tectonically controlled with extension normal to the rift flanks as is the case of Albertine, Kivu or North Tanganyika Rifts. In the case of the Rukwa Rift and along the Eastern Branch particularly in the Manyara Rift, rifting is magmatically controlled. Here, the extension direction given by seismic studies, the morphology of the rift flanks and kinematic analyses indicate rifting is oblique to the direction of relative tectonic motion. This can be interpreted as the result of changes in the local stress field generated by magmatic injection. South of 3° S, where magmatic processes are less pronounced, the tectonic boundary becomes more complex, forming a boundary area, with an outer limit that we suggest that follows a slow right-lateral transform that joins Kerimbass Rift in the offshore.

ACKNOWLEDGMENTS

Most of the figures were prepared with Mirone suite (Luis 2007) and GMT software tools (Wessel & Smith 1998). The research presented here was funded by the Portuguese Science Foundation KINEMA project (PTDC/CTE-GIN/64101/2006). DD was supported by the Belgian Science Policy under the Action 1 programme. DSS was funded by the National Science Foundation Graduate Research Fellowship Programme.

REFERENCES

- Albaric, J., Déverchère, J., Petit, C., Perrot, J. & Le Gall, B., 2009. Crustal rheology and depth distribution of earthquakes: insights from the central and southern East African Rift System, *Tectonophysics*, **468**(1–4), 28–41.
- Altamimi, Z., Collilieux, X. & Métivier, L., 2011. ITRF2008: an improved solution of the international terrestrial reference frame, *J. Geod.*, **85**(8), 457–473.
- Argus, D.F., Gordon, R.G., Heflin, M.B., Ma, C., Eanes, R.J., Willis, P., Peltier, W.R. & Owen, S.E., 2010. The angular velocities of the plates and the velocity of the Earth's centre from space geodesy, *Geophys. J. Int.*, **18**, 1–48.
- Blewitt, G., 2008. Fixed point theorems of GPS carrier phase ambiguity resolution and their application to massive network processing: Ambizap, *J. geophys. Res.*, **113**(B12410), doi:10.1029/2008JB005736.
- Blewitt, G. & Lavalley, D., 2002. Effect of annual signals on geodetic velocity, *J. geophys. Res.*, **107**(B7), doi:10.1029/2001JB000570.
- Bos, M.S., Fernandes, R.M.S., Williams, S.D.P. & Bastos, L., 2008. Fast error analysis of continuous GPS observations, *J. Geod.*, **82**, 157–166.
- Brazier, R.A., Nyblade, A.A. & Florentin, J., 2005. Focal mechanisms and the stress regime in NE and SW Tanzania, East Africa, *Geophys. Res. Lett.*, **32**, doi:10.1029/2005GL023156.
- Calais, E., Ebinger, C.J., Hartnady, C. & Nocquet, J.M., 2006. Kinematics of the East African Rift from GPS and earthquake slip vector data, in *The Afar Volcanic Province within the East African Rift System*, Vol. **259**, pp. 9–22, eds Yirgu, G., Ebinger, C.J. & Maguire, P.K.H., Geol. Soc. Spec. Publ.
- Calais, E. *et al.*, 2008. Strain accommodation by slow slip and dyking in a youthful continental rift, East Africa, *Nature*, **456**, 783–787.
- Corti, G., 2009. Continental rift evolution: from rift initiation to incipient break-up in the Main Ethiopian Rift, East Africa, *Earth-Sci. Rev.*, **96**, doi:10.1016/j.earscirev.2009.06.005.
- Delvaux, D., 2001. Tectonic and palaeostress evolution of the Tanganyika-Rukwa-Malawi rift segment, East African Rift System, *Mem. Mus. Natn. Hist. Nat.*, **186**, 545–567.
- Delvaux, D. & Barth, A., 2010. African stress pattern from formal inversion of focal mechanism data. Implications for rifting dynamics, *Tectonophysics*, **482**, 105–128.
- Delvaux, D., Levi, K., Kajara, R. & Sarota, J., 1992. Cenozoic paleostress and kinematic evolution of the Rukwa: North Malawi rift valley (East African rift system), *Bull. Cent. Rech. Explor.-Prod. Elf Aquitaine*, **16**(2), 383–406.
- Delvaux, D., Kervyn, F., Macheyeki, A.S. & Temu, E.B., 2012. Geodynamic significance of the TRM segment in the East African Rift (W-Tanzania): active tectonics and paleostress in the Ufipa plateau and Rukwa basin, *J. Struct. Geol.*, **37**, 161–180.
- DeMets, C., Gordon, R.G., Argus, D.F. & Stein, S., 1990. Current plate motions, *Geophys. J. Int.*, **101**, 425–478.
- Ebinger, C., 1989. Tectonic development of the Western Branch of the East African rift system, *Geol. Soc. Am. Bull.*, **101**, 885–903.
- Ebinger, C., Yemane, T., WoldeGabriel, G., Aronson, J. & Walter, R., 1993. Eocene: recent volcanism and faulting in the southern Main Ethiopian Rift, *J. Geol. Soc., Lond.*, **150**, 99–108.
- Fernandes, R.M.S., Ambrosius, B.A.C., Noomen, R., Bastos, L., Combrinck, L., Miranda, J.M. & Spakman, W., 2004. Angular velocities of Nubia and Somalia from continuous GPS data: implications on present-day relative kinematics, *Earth planet. Sci. Lett.*, **222**, 197–208.
- Foster, A. & Jackson, J.A., 1998. Source parameters of large African earthquakes: implications for crustal rheology and regional kinematics, *Geophys. J. Int.*, **134**, 422–448.
- George, R., Rogers, N. & Kelley, S., 1998. Earliest magmatism in Ethiopia: evidence for two mantle plumes in one flood basalt province, *Geology*, **26**, 923–926.
- Global CMT, 2011. Available at: <http://www.globalcmt.org>, accessed 2011 October 5.
- Hartnady, C.J.H., 2002. Earthquake hazard in Africa: perspectives on the Nubia-Somalia boundary, *S. Afr. J. Sci.*, **98**, 425–428.
- Horner-Johnson, B.C., Gordon, R.G. & Argus, D.F., 2007. Plate kinematic evidence for the existence of a distinct plate between the Nubian and Somalian plates along the Southwest Indian Ridge, *J. geophys. Res.*, **112**, doi:10.1029/2006JB004519.
- IRIS, 2011. Available at <http://www.iris.edu>, accessed 2011 October 5.
- Kaz'min, V.G., Zonenshayn, L.P., Savostin, L.A. & Bershbitskaya, A.I., 1987. Kinematics of the Afro-Arabian Rift System, *Geotectonics*, **21**, 452–460.
- LeGall, B. *et al.*, 2004. Neogene-Recent rift propagation in Central Tanzania: morphostructural and aeromagnetic evidence from the Kilombero area, *Geol. Soc. Am. Bull.*, **116**, 490–510.

- Lindenfeld, M. & Rumpker, G., 2011. Detection of mantle earthquakes beneath the East African Rift, *Geophys. J. Int.*, **186**, doi:10.1111/j.1365-246X.2011.05048.x.
- Luis, J.F., 2007. Mirone: a multi-purpose tool for exploring grid data, *Comput. Geosci.*, **33**, 31–41.
- Luis, J.F. & Miranda, J.M., 2008. Reevaluation of magnetic chrons in the North Atlantic between 35°N and 47°N: implications for the formation of the Azores Triple Junction and associated plateau, *J. geophys. Res.*, **113**(B10105), doi:10.1029/2007JB005573.
- Macheyeki, A.S., Delvaux, D., DeBatist, M. & Mruma, A., 2008. Fault kinematics and tectonic stress in the seismically active Manyara–Dodoma Rift segment in Central Tanzania: implications for the East African Rift, *J. Afr. Earth Sci.*, **51**, 163–188.
- Nicholas, A., Achauer, U. & Daigieres, M., 1994. Rift initiation by lithospheric rupture, *Earth planet. Sci. Lett.*, **123**(1–3), 281–298.
- Prawirodirdjo, L. & Bock, Y., 2004. Instantaneous global plate motion model from 12 years of continuous GPS observations, *J. geophys. Res.*, **109**, doi:10.1029/2003JB002944.
- Rebischung, P., Griffiths, J., Ray, J., Schmid, R., Collilieux, X. & Garayt, B., 2011. IGS08: the IGS realization of ITRF2008, *GPS Solutions*, doi:10.1007/s10291-011-0248-2.
- Roberts, E.M. *et al.*, 2012. Initiation of the Western Branch of the East African Rift coeval with the Eastern Branch, *Nat. Geosci.*, **5**, 289–294.
- Sella, G.F., Dixon, T.H. & Mao, A., 2002. REVEL: a model for recent plate velocities from space geodesy, *J. geophys. Res.*, **107**, 1–30.
- Stamps, D.S., Calais, E., Saria, E., Hartnady, C., Nocquet, J.-M., Ebinger, C.J. & Fernandes, R.M., 2008. A kinematic model for the East African Rift, *Geophys. Res. Lett.*, **35**(L05304), doi:10.1029/2007GL032781.
- Webb, F. & Zumberge, J., 1995. An introduction to GIPSY/OASIS-II, Tech. Rep., JPL D-11088, California Institute of Technology, Pasadena, California.
- Weeraratne, D.S., Forsyth, D.W. & Fischer, K.M., 2003. Evidence for an upper mantle plume beneath the Tanzania Craton from Rayleigh wave tomography, *J. geophys. Res.*, **108**(B9), 2427, doi:10.1029/2002JB002273.
- Wessel, P. & Smith, W.H.F., 1998. New, improved version of the Generic Mapping Tools released, *EOS, Trans. Am. geophys. Un.*, **79**, 579.
- Yang, Z. & Chen, W.-P., 2010. Earthquakes along the East African Rift System: a multiscale, system-wide perspective, *J. geophys. Res.*, **115**, doi:10.1029/2009JB006779.
- Zumberge, J., Heflin, M., Jefferson, D., Watkins, M. & Webb, F., 1997. Precise Point Positioning for the efficient and robust analysis of GPS data from large networks, *J. geophys. Res.*, **102**, 5005–5017.

SUPPORTING INFORMATION

Additional Supporting Information may be found in the online version of this article:

- Figure S1.** De-trended time-series for ELDS (Victoria Block).
Figure S2. De-trended time-series for KISM (Somalia Plate).
Figure S3. De-trended time-series for KSMU (Victoria Block).
Figure S4. De-trended time-series for MAL2 (Somalia Plate).
Figure S5. De-trended time-series for MALI (Somalia Plate).
Figure S6. De-trended time-series for MBAR (Victoria Block).
Figure S7. De-trended time-series for MOIU (Victoria Block).
Figure S8. De-trended time-series for MOSH.
Figure S9. De-trended time-series for NURK (Victoria Block).
Figure S10. De-trended time-series for RCMN (Somalia Plate).
Figure S11. De-trended time-series for REUN (Somalia Plate).
Figure S12. De-trended time-series for SCTR (Somalia Plate).
Figure S13. De-trended time-series for SEY1 (Somalia Plate).
Table S1. List of the stations excluded for the final computation of the angular velocities for Nubia.
Table S2. List of the stations excluded for the final computation of the angular velocities for Somalia (<http://gji.oxfordjournals.org/lookup/supp1/doi:10.1093/gji/ggs071/-/DC1>).

Please note: Oxford University Press is not responsible for the content or functionality of any supporting materials supplied by the authors. Any queries (other than missing material) should be directed to the corresponding author for the article.